Cell

Cryo-EM Reconstruction of Dengue Virus in Complex with the Carbohydrate Recognition Domain of DC-SIGN

Elena Pokidysheva,[1] Ying Zhang,[1] Anthony J. Battisti,[1] Carol M. Bator-Kelly,[1] Paul R. Chipman,[1] Chuan Xiao,[1] G. Glenn Gregorio,[2] Wayne A. Hendrickson,[2] Richard J. Kuhn,[1] and Michael G. Rossmann[1,*]
[1] Department of Biological Sciences, Lilly Hall, 915 W. State Street, Purdue University, West Lafayette, IN 47907, USA
[2] Department of Biochemistry and Molecular Biophysics, Howard Hughes Medical Institute, Columbia University, New York, NY 10032, USA
*Contact: mr@purdue.edu
DOI 10.1016/j.cell.2005.11.042

SUMMARY

Dengue virus (DENV) is a significant human pathogen that causes millions of infections and results in about 24,000 deaths each year. Dendritic cell-specific ICAM3 grabbing nonintegrin (DC-SIGN), abundant in immature dendritic cells, was previously reported as being an ancillary receptor interacting with the surface of DENV. The structure of DENV in complex with the carbohydrate recognition domain (CRD) of DC-SIGN was determined by cryo-electron microscopy at 25 Å resolution. One CRD monomer was found to bind to two glycosylation sites at Asn67 of two neighboring glycoproteins in each icosahedral asymmetric unit, leaving the third Asn67 residue vacant. The vacancy at the third Asn67 site is a result of the nonequivalence of the glycoprotein environments, leaving space for the primary receptor binding to domain III of E. The use of carbohydrate moieties for receptor binding sites suggests a mechanism for avoiding immune surveillance.

INTRODUCTION

Dengue virus (DENV), belonging to the flavivirus genus of the *Flaviviridae* family, is an arthropod-borne human pathogen, causing more than 50 million human infections each year (Lindenbach and Rice, 2001). Sequential infections by any of the four DENV serotypes can cause severe symptoms, such as dengue hemorrhagic fever and dengue shock syndrome, probably via antibody-dependent enhancement (ADE) (Morens, 1994). Thus, it is necessary to block infection by all four DENV serotypes if secondary infections due to ADE are to be avoided. Therefore, the development of vaccines against dengue virus is a nontrivial issue.

Mature DENV is roughly spherical and approximately 500 Å in diameter (Kuhn et al., 2002; Zhang et al., 2003a). There are three structural proteins, the envelope (E) protein, membrane protein, and capsid protein, present in mature virions. The crystal structure of the E protein showed that it has three domains, the N-terminal structurally central domain I, the dimerization domain II, and the C-terminal, Ig-like domain III (Rey et al., 1995; Modis et al., 2003; Zhang et al., 2004). By combining cryo-electron microscopy (cryoEM) results with the crystal structure of the E protein, it was shown that the icosahedral asymmetric unit consists of three E monomers (Kuhn et al., 2002; Zhang et al., 2003a). One monomer, together with its icosahedral 2-fold related counterpart, forms an ''icosahedral dimer.'' The other two monomers form a dimer at a general position (the ''general dimer''). Two potential N-linked carbohydrate sites, at Asn67 and Asn153, are both glycosylated in DENV serotype 2 (DENV2) (strain PR159-S1), but in the homologous West Nile virus (WNV) there is only one glycosylation site at residue Asn154 (Mukhopadhyay et al., 2003; Zhang et al., 2003a). A difference cryoEM map between DENV2 and WNV established the locations of the carbohydrate sites in these viruses, which were found to be consistent with the fitting of the E proteins. The E protein undergoes significant conformational changes, centered around a hinge between domains I+III and domain II, during the viral life cycle (Zhang et al., 2003b; Zhang et al., 2004).

DENV is transmitted between humans via mosquito vectors (Lindenbach and Rice, 2001). Immature dendritic cells (DCs) and Langerhans cells, resident in skin, are the initial target cells of DENV infection (Wu et al., 2000). DENV enters these cells via receptor-mediated endocytosis (Lindenbach and Rice, 2001). However, the primary receptors of DENV are still unknown. Recent studies have shown that DENV infection can be inhibited by soluble extracellular *d*endritic *c*ell-*s*pecific *I*CAM3 *g*rabbing *n*onintegrin (DC-SIGN) as well as by antibodies against DC-SIGN (Navarro-Sanchez et al., 2003; Tassaneetrithep et al., 2003). This suggests an essential role of DC-SIGN in the DENV infection of immature DCs. However, the endocytosis of DC-SIGN itself is not required for the internalization of DENV into cells (Lozach et al., 2005).

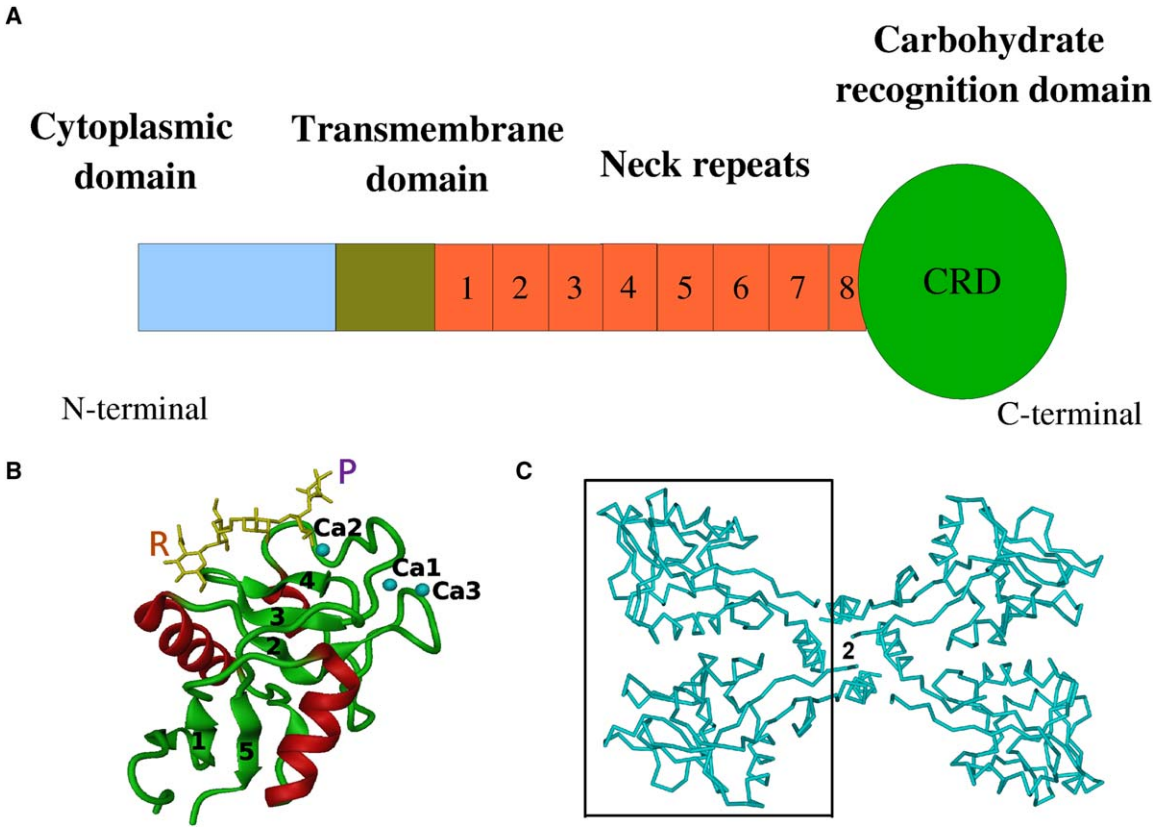

Figure 1. Structure of DC-SIGN

(A) Schematic diagram showing the domain composition of DC-SIGN.

(B) The crystal structure of the CRD monomer (PDB accession number 1K9I) is shown as a ribbon diagram. The bound oligosaccharide (GlcNAc-mannose$_3$-GlcNAc) is represented in yellow, three bound Ca^{2+} ions in blue, the α helices in red, and the remainder of the structure, including the two principal β sheets, in green. The approximate binding site of the carbohydrates associated with Asn67 in the red and purple molecules (Figure 2B) are marked R and P, respectively.

(C) The C_α backbone traces of the DC-SIGNR tetrameric fragment (PDB accession number 1XAR). The crystallographic 2-fold axis is marked with a "2". The dimer used for fitting into a single cryoEM difference peak is outlined with a rectangular black box (Table 2).

DC-SIGN, a carbohydrate binding, C-type, lectin-like molecule, is involved in cell adhesion but can also function as a phagocytic pathogen-recognition receptor in the immune system (Cambi and Figdor, 2003). Nevertheless, DC-SIGN can be used as the binding target prior to cell entry by many viral pathogens, including hepatitis C virus and human immunodeficiency virus (Lozach et al., 2003; Su et al., 2004). DC-SIGN is composed of a cytoplasmic domain, a transmembrane domain, an extracellular neck domain of eight tandem 23-amino acid residue repeats, and a carbohydrate recognition domain (CRD) (Figure 1). DC-SIGN is a tetramer on DC surfaces (Bernhard et al., 2004) formed by the neck domain repeats, whereas isolated CRDs are monomeric (Mitchell et al., 2001). The C-terminal CRD of DC-SIGN is responsible for recognition of high mannose glycans in the presence of Ca^{2+} (Mitchell et al., 2001; Guo et al., 2004). Various crystal structures of fragments of DC-SIGN and DC-SIGN relatives (DC-SIGNR), which have ~80% sequence identity to DC-SIGN, have been determined in complex with a variety of carbohydrate ligands (Feinberg et al., 2001, 2005; Guo et al., 2004; Snyder et al., 2005). These show that the CRD has the characteristic C-type lectin fold (Weis et al., 1991), a mixed α/β structure with two primary antiparallel β sheets. Several loops are clustered at one face of the CRD, forming the oligosaccharide binding site that is away from the N and C termini (Figure 1B).

A number of structures are available of viral components that are complexed with relevant fragments of cellular receptors (Stehle and Harrison, 1996, 1997; Kwong et al., 1998; Bewley et al., 1999; Carfi et al., 2001; Burmeister et al., 2004). These have been determined almost exclusively by X-ray crystallography to near atomic resolution. Fewer structural investigations exist of whole viruses complexed with their cellular protein receptors. Most, but not all (Verdaguer et al., 2004), of these utilize cryoEM because of the difficulty of crystallizing such convoluted objects and because of their tendency to be unstable. The large majority of the virus-receptor complex studies are of picornaviruses, including human rhinoviruses, polioviruses, coxsackieviruses, foot-and-mouth disease viruses, and echoviruses (Rossmann

et al., 2002). The instability of virus-receptor complexes is the result not only of weak affinity between the virus and receptor but also the fact that recognition of a host cell by a virus initiates cell entry and uncoating of the viral capsid to release the genome. Picornaviruses, unlike DENV, do not have a lipid envelope nor are their surfaces glycosylated, making virus-receptor recognition dependent mostly on protein-protein interactions.

We report here the cryoEM reconstruction of DENV2 in complex with the CRD of human DC-SIGN at 25 Å resolution. This is the first structural investigation of an intact lipid-enveloped virus interacting with a protein receptor molecule that recognizes a specific site on the virus surface. The structure shows that monomeric CRD of DC-SIGN binds to the N-linked glycans at Asn67 of each of two neighboring E proteins. The N termini of CRDs in intact DC-SIGN connect to the cell membrane through the tetrameric neck segment. The termini of two adjacent, icosahedral, 2-fold-related CRDs are close to each other, possibly making a complex as suggested by a tetrameric model of DC-SIGN (Feinberg et al., 2005; Snyder et al., 2005).

RESULTS AND DISCUSSION

Structure of the DENV-CRD Complex

The biological activity of the refolded CRD of DC-SIGN, expressed in *E. coli,* was verified by an ELISA experiment that determined the binding affinity of the CRD to DENV (Table 1). This demonstrated that the DC-SIGN sample was able to bind to DENV (see Experimental Procedures). The 25 Å resolution cryoEM reconstruction of the DENV-CRD complex showed 60 icosahedrally arranged protrusions on the external surface of DENV (Figure 2A). These protrusions were at 3.6 σ above the mean and were the highest peak in a difference map of the complex minus DENV. The next highest peak located outside the E protein shell was 2.2 σ. Thus, these protrusions are probably CRD molecules bound to DENV. The height of the density corresponding to the CRD molecules is about half of the densities of the E glycoproteins in the cryoEM reconstruction of the complex. Hence, some of the CRD binding sites are probably unoccupied, or the CRD molecules have considerable variation in their position on the viral surface. Fitting the known atomic structure of one CRD monomer into a single protrusion of the difference map gave a far better result as determined by the parameters shown in Table 2 than fitting of two closely packed CRD monomers into the same density.

The orientation and position of E dimers fitted into the cryoEM map of the complex were similar to the E dimers fitted into a 25 Å resolution cryoEM reconstruction of mature DENV (Table 3), showing that the E molecule does not undergo any significant conformational changes on binding to CRD. This might be because DC-SIGN is merely an attachment receptor and probably functions to concentrate viruses on cell membranes rather than being the mediator required for subsequent endocytosis of DENV into cells (Lozach et al., 2005). However, DC-SIGN is essential for DENV infection of immature DCs (Navarro-Sanchez et al., 2003; Tassaneetrithep et al., 2003; Lozach et al., 2005). Thus, it is possible that binding of full-length DC-SIGN, as opposed to CRD alone, might trigger changes on the virus or initiate clustering of a yet unidentified primary receptor molecule, leading to endocytosis.

Table 1. Binding Activity of Recombinant DC-SIGN CRD to DENV as determined by an Elisa Experiment

DC-SIGN CRD + DENV+ (Positive Test)	DC-SIGN CRD+ DENV− (Negative Control 1)	DC-SIGN CRD − DENV+ (Negative Control 2)
0.37 ± 0.08	0.08 ± 0.05	0.05 ± 0.05

The values shown are average optical densities measured at 405 nm for three experiments.

Location of the CRD in the Complex

CRD binds mannose with high affinity compared to other types of sugar moieties (Guo et al., 2004). Furthermore, the carbohydrates on the E protein are high in mannose content (Johnson et al., 1994), suggesting that DC-SIGN might bind to the carbohydrate moieties on DENV (Navarro-Sanchez et al., 2003; Tassaneetrithep et al., 2003). The CRD monomer was restrained to fit into the cryoEM difference map so as to place the oligosaccharide binding region as close to the viral surface and in a manner consistent with a good fit. This placed the CRD molecule close to two of the glycosylated residues on the viral surface. One of these sites was Asn67 in the molecule belonging to the icosahedral dimer (red in Figure 2B), and the other was Asn67 in the adjacent molecule (purple in Figure 2B) belonging to the general dimer. The distances between the center of the oligosaccharide bound to the CRD and the two Asn67s are 15 and 18 Å, comparable to distances found in a study of carbohydrate sites in Sindbis virus (Pletnev et al., 2001). The third Asn67 site is empty, as are all Asn153 sites. Therefore, CRD of DC-SIGN apparently interacts with DENV by binding the CRD to carbohydrate moieties located on Asn67 in two neighboring E molecules. This is consistent with Asn67, but not with Asn153, being conserved in all four serotypes of DENV, all of which utilize DC-SIGN for infecting immature DCs (Lozach et al., 2005). In addition, mutagenesis studies have shown that Asn67 is essential and sufficient for DENV infection of immature DCs, whereas mutating Asn153 produces only a mild reduction in virus infectivity (C. Blair, J. Roehrig, C. Huang, S. Butrapet, and R. Kinney, personal communication).

Each icosahedral asymmetric unit of DENV2 contains six glycosylation sites, three Asn67s, and three Asn153s. However, CRD only binds to two out of the three Asn67 sites and not to any of the Asn153 sites, although CRD was present in considerable excess (see Experimental Procedures). The absence of bound CRD at other carbohydrate moieties is unlikely to be the result of steric hindrance between CRD and the E protein because the carbohydrates are fully exposed

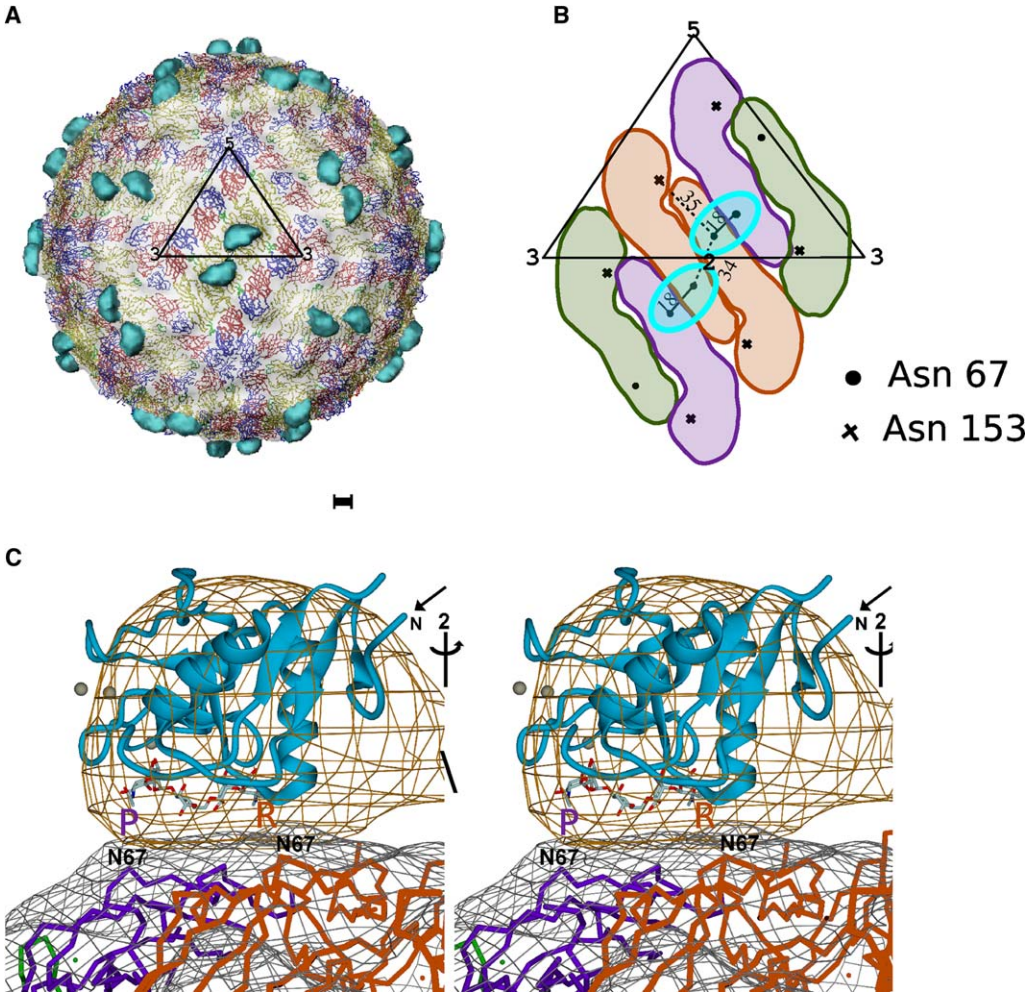

Figure 2. The Structure of the DENV-CRD Complex

(A) Surface-shaded representation of the DENV-CRD complex at 25 Å resolution. The C_α backbone traces of the fitted E dimers are shown with domains I, II, and III colored in red, yellow, and blue, respectively. The bound CRD molecules are shaded in cyan. An icosahedral asymmetric unit is outlined in black. Scale bar represents 50 Å.

(B) Schematic diagram showing positions of the N-linked glycosylation sites, Asn67 (●) and Asn153 (X). Distances between closest sugar atoms of neighboring sites are shown. The boundaries of the E dimers and the corresponding CRD (cyan) are shown. The icosahedral dimer is in red, whereas the two molecules of the general dimer are in purple and green. An icosahedral asymmetric unit is outlined in black.

(C) Stereo diagram showing the side view of the fitted CRD and DENV E proteins. The C_α backbone trace of the DENV E proteins and the ribbon diagram of the fitted structure of CRD (cyan) are shown in the difference map (light brown) at a contour level of 2.4 σ. The outline of a 14 Å resolution map of DENV (gray) indicates the position of the carbohydrate sites. The icosahedral 2-fold symmetry axis is also shown. The termini of the CRDs are labeled "N". The oligosaccharide ligands and calcium atoms associated with the crystal structure of CRD are shown in ball-and-stick format to indicate the location of the carbohydrate binding site on the CRD. The approximate sites for the carbohydrate moieties associated with the red and purple molecules in Figure 2B are marked R and P, respectively. The C_α atoms of Asn67s are labeled.

on the viral surface (Modis et al., 2003; Zhang et al., 2003a; Zhang et al., 2004). Nor is it likely that there would be steric hindrance between other potential binding sites and the observed sites because their separation is more than the diameter of the CRD monomer and because such a situation would likely result in partial occupancy of all possible sites.

The closest distance between atoms of the first sugar residues attached to the two Asn67s that bind to the same CRD is ~18 Å, shorter than that between any other two neighboring carbohydrate sites on the viral surface (Figure 2B). One CRD molecule would not be able to bind to any other pair of glycosylation sites, as their separation would be too large. The affinity of CRD to carbohydrates increases with the number of mannose moieties in the oligosaccharide (Lozach et al., 2003), lending plausibility to the binding of DC-SIGN CRD to two glycosylation sites on DENV. Although the binding of a single C-type lectin CRD to two carbohydrate moieties is unprecedented, DC-SIGN has an extended carbohydrate binding region (Figure 1B) with a subsite 9–12 Å away from the principal Ca^{2+}-mediated site (Feinberg et al., 2001),

Table 2. Fitting of the CRD Monomers and the Dimer into the Difference Map between the DENV-CRD Complex and DENV

Model	*Sumf*[a]	*Clash*[a]	*-Den*[a]	Center (Å)		
				x^a	y^a	z^a
One CRD Monomer (1K9I)[b]	52.7	0.0	0.0	22.7	−11.6	255.3
Two CRD Monomers (1K9I)[c]	46.1	7.8	52.0	20.2	−14.1	250.8
Two CRD Monomers (1XAR)[d]	47.0	0.0	47.0	23.7	−7.6	248.8

[a] Parameters are described in detail in the paper by Rossmann et al. (Rossmann et al., 2001). *Sumf* is defined as the average value of density for all nonhydrogen atomic positions normalized by setting the highest density in the map to 100; *Clash* represents the percentage of atoms in the model that have steric clashes with symmetry-related subunits; *–Den* denotes the percentage of atoms that are positioned in negative density; and *x*, *y*, and *z* are the three translational parameters describing the position of the mass center of the fitted model.
[b] The structure of one CRD monomer of crystallized DC-SIGN CRD (PDB accession number 1K9I) was used for fitting.
[c] The structure of the two closest CRD monomers in one asymmetric unit of crystallized DC-SIGN CRD (PDB accession number 1K9I) was used for fitting.
[d] The CRD dimer, taken from the crystal structure of the tetramer of the DC-SIGNR (PDB accession number 1XAR), selected as shown by the black rectangle in Figure 1C.

and the CRD fitted into density on the virus has these two subsites directed toward the two apposed Asn67 residues. Apparently, the peculiar geometry of the paired Asn67 glycosylation sites in neighboring red and purple molecules on DENV (Figure 2B) is necessary to obtain a stable complex between CRD and the virus. The alternative interpretation that the CRD binds to only one Asn67 residue at a time, yielding averaged density from two overlapping states, is implausible since the single Asn67 site on the green monomer (Figure 2B) is unoccupied. One could imagine different sugar moieties on Asn67 and Asn153, with only the former recognized by CRD, but all Asn67 sites should be glycosylated in the same manner.

The N termini of the CRDs are brought together by the tetrameric neck repeats as found in a crystalline tetrameric association of two-repeat fragments (Feinberg et al., 2005). In the DENV-CRD complex, the N termini of adjacent 2-fold-related CRDs face each other (Figure 2B). Furthermore, the distance between the centers of these fitted CRDs is 51 Å, similar to the 54 Å distance between the 2-fold-related CRDs in the crystal structure of the tetramer (Feinberg et al., 2005). These results imply that the two adjacent CRDs on the viral surface could be part of a tetrameric, full-length DC-SIGN when binding to DENV (Figure 3, Table 2), in agreement with the binding affinity between DC-SIGN and DENV being greater for the tetrameric form than for the monomeric form (Lozach et al., 2005). However, the relative orientation of one CRD molecule with respect to the other as observed here on the DENV surface differs from that observed in the crystal structure of tetrameric DC-SIGNR fragments (Figure 3). This may be due to the flexibility of the junction between the CRD and the neck repeat region of DC-SIGNR (Feinberg et al., 2005; Snyder et al., 2005) or due to the uncertainty of fitting a somewhat globular CRD structure into the also somewhat distorted spherical density. Thus, the binding of the two adjacent CRD molecules to DENV probably mimics the interaction between DENV and DC-SIGN on DCs in vivo.

Biological Implications

The structure of flaviviruses, such as DENV, is unusual in that in each icosahedral asymmetric unit there are three covalently identical E glycoprotein molecules (Kuhn et al., 2002) that do not obey the rules of quasi-symmetry proposed by Caspar and Klug (Caspar and Klug, 1962). The resultant different environment of each of the three E molecules permits

Table 3. Fitting of the E Dimers into the DENV-CRD Complex and into Mature DENV Maps at 25 Å Resolution

Map	Model	*Sumf*[a]	*Clash*[a]	*-Den*[a]	Orientation (°)			Center (Å)			Radius[b]
					θ_1	θ_2	θ_3	x^a	y^a	z^a	
Complex	Icosahedral Dimer	70.7	0.0	0.0	−0.2	0.0	0.0	0.0	0.0	220.5	220.5
	General Dimer	78.4	0.8	0.8	43.5	46.8	135.0	43.8	−31.1	211.0	217.7
DENV	Icosahedral Dimer	60.8	0.0	4.4	1.8	0.0	0.0	0.0	0.0	219.5	219.5
	General Dimer	60.7	0.7	3.4	45.0	45.0	135.0	42.8	−31.1	210.0	216.6

[a] Parameters are described in Table 2.
[b] The radius of the mass center of the fitted E dimer in the virus particle after the magnification of the complex map was adjusted (see Experimental Procedures).

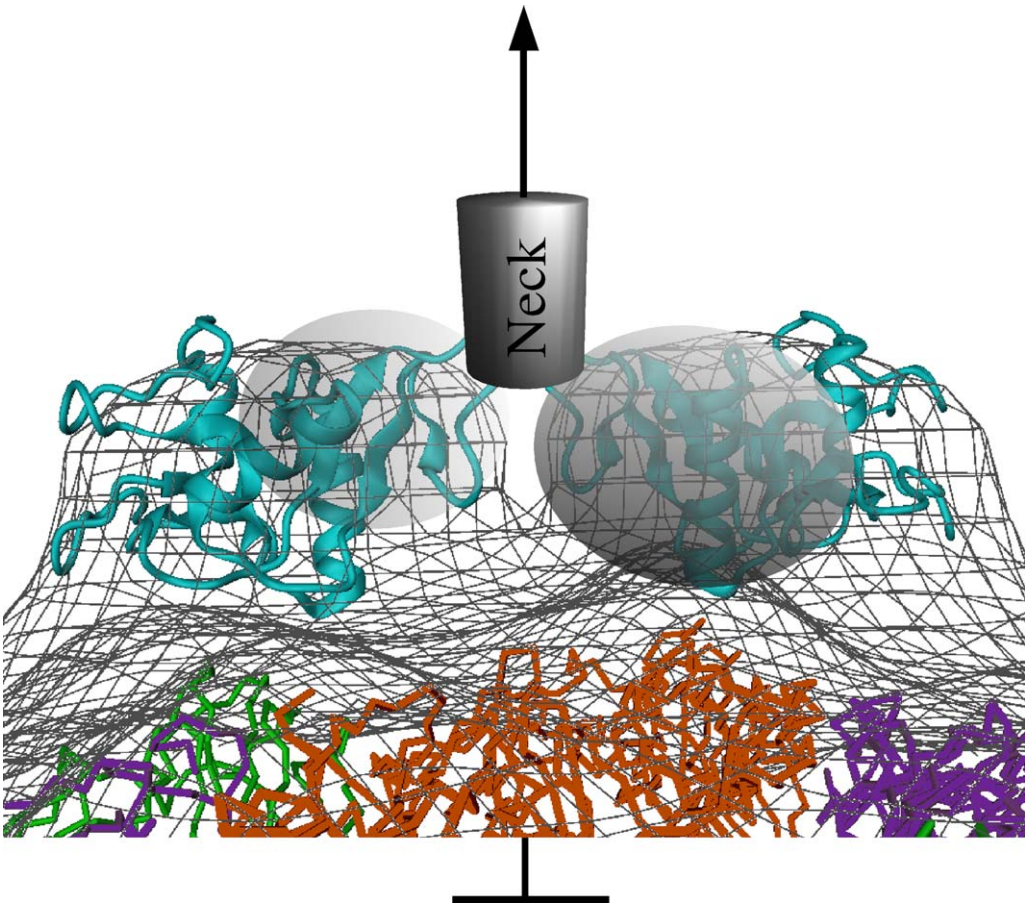

Figure 3. Diagrammatic Representation of a DC-SIGN Tetrameric Molecule Interacting with the DENV Surface

The DC-SIGN CRD domains are represented by the blue ribbon molecules bound at 2-fold related sites on the virus. The two other CRD domains and the joining neck region are represented by the gray shaded areas. The E proteins on the surface of the virus are shown by the virtual bonds between the C_α atoms using the same color code for the different E subunits as were used in Figure 2B. The cryoEM density is represented by a chicken-wire mesh colored black.

one CRD to bind to two of the three E molecules, leaving the third unassociated. As a result, there is space on the viral surface for the primary receptor that probably binds to domain III of the E proteins (Rey et al., 1995; Bhardwaj et al., 2001). There are three clusters of domain III. The first is immediately around the 5-fold vertices, the second forms an outer ring around the 5-fold cluster, and the third forms a cluster around the 3-fold axes. Binding of DC-SIGN to the Asn67 residues on the red and purple molecules would leave the 5-fold cluster well exposed. Furthermore, binding of a number of DC-SIGN molecules to the virus surface would create a lattice or cluster in the cell membrane that might signal recruitment of the primary receptor molecules in preparation for subsequent endocytosis.

There is a parallel to the use of DC-SIGN as an ancillary receptor for DENV with the use of decay accelerating factor (DAF, CD55) as an ancillary receptor by some picornaviruses. Both DC-SIGN and DAF can enhance infectivity without promoting cell entry. Furthermore, in the same way that DC-SIGN leaves ample space on the DENV surface for the binding of a primary receptor, when DAF binds to various picornaviruses (He et al., 2002; Bhella et al., 2004), it does so well away from the "canyon," the site on picornavirus surfaces associated with the primary receptor binding.

It has been proposed that rhino-, entero-, and picornaviruses escape immune surveillance by hiding their receptor attachment site in a "canyon" on the viral surface that is in part inaccessible to neutralizing antibodies (Rossmann et al.,1985; Rossmann, 1994). In the present case, the receptor binds to a protrusion created by carbohydrate moieties rather than a depression created by a rigid protein structure. As the host has glycosylated not only the viral proteins but many other cellular proteins, its immune system is unlikely to react to the viral carbohydrate sites, thereby providing a different mechanism to bypass the host's immune protection. The function of DC-SIGN is to be able to bind to diverse mannose structures, a feat not normally accomplished by a specific antibody.

EXPERIMENTAL PROCEDURES

Preparation of DENV and CRD of DC-SIGN

DENV2 virus, strain PR159-S1, was grown and purified as described previously (Kuhn et al., 2002). The antifungal agent Ketoconazole (Sigma), at a final concentration of 5 μg/ml, was used to increase the virus yield. The purified virus was maintained in a buffer containing 50 mM Tris (pH 7.5), 75 mM NaCl, and 1 mM EDTA at 4ºC.

The CRD of human DC-SIGN was refolded from inclusion bodies produced in *Escherichia coli*. A cDNA corresponding to the CRD (Arg251-Ala404) was cloned into an expression vector that also generates 20 additional N-terminal residues, including a hexahistidine tag and a thrombin cleavage site. Recombinant protein expressed from *E. coli* BL21-DE3 cells (Novagen) transfected with this vector aggregated into inclusion bodies. Washed inclusion bodies were solubilized in 6 M guanidine HCl, pH 8.0, and refolded by dilution at 4ºC to a final concentration of 1 mg/ml in a refolding buffer (550 mM guanidine HCl, 550 mM L-arginine, 55 mM Tris, pH 8.2, 10.6 mM NaCl, 2.2 mM $MgCl_2$, 2.2 mM $CaCl_2$, 1 mM reduced glutathione (GSH), 0.1 mM oxidized glutathione [GSSG]) and subsequent dialysis (20 mM Tris, pH 8.0, 50 mM NaCl). The refolded protein was purified by Ni-column chromatography. No attempt was made to remove the his tag from the protein.

The biological function of the refolded protein was partially verified by ELISA. Purified CRD (100 μl at the concentration of 5 μM in borate saline buffer at pH 9) was incubated for 12 hr at 4ºC on 96-well Immulon 2 U-bottom plates (Dynatech). Plates were then blocked with 20 mM Tris (pH 7.5), 100 mM NaCl, 5% milk, and 5 mM Ca^{2+} for 2 hr at room temperature to avoid nonspecific binding, followed by three steps of washing with buffer containing 0.1% of Tween-20. Purified DENV (10 μg/ml in 20 mM Tris, pH 7.5, 100 mM NaCl, and 5 mM Ca^{2+}), corresponding to 20 mM E protein, was added to the wells for 2 hr at room temperature. Bound DENV was then detected with primary monoclonal anti-E (9A3D-8) and secondary anti-mouse horseradish peroxidase (HRP)-conjugated antibodies. HRP activity was detected by measuring the optical density at 405 nm using TMB Microwell Peroxidase Substrate System (KPL Reagents, Inc.). Negative controls included the omission of the virus or CRD.

CryoEM and Image Processing

Purified DENV was mixed with CRD of DC-SIGN to the final concentration of 0.5 mg/ml and 5 mg/ml, respectively, giving a ratio of 30 CRD molecules per E protein. The sample also contained 10 mM $CaCl_2$ and was incubated at 4ºC for about 12 hr.

The vitrified water-embedded sample (Figure 4) was examined with an FEI CM300 field emission gun transmission electron microscope under low-dose conditions (11.8 electrons/$Å^2$) at a magnification of 33,000. The micrographs were digitized using a pixel size of 4.24 Å with a Zeiss Phodis SCSI scanner. Particles were boxed, and the defocus level was estimated using the program RobEM (http://bilbo.bio.purdue.edu/~workshop/help_robem). A total of 830 particles were selected from 45 micrographs taken with defocus levels ranging from 1 μm to 3 μm, although the majority of micrographs were close to 3 μm out-of-focus. The scanned raw images were corrected with the phase contrast transfer function according to the procedure described by Conway and Steven (Conway and Steven, 1999). The cryoEM reconstruction of DENV2 (Zhang et al., 2003a) was used as the initial model to perform the three-dimensional reconstruction using the projection-matching procedure with the SPIDER program (Frank et al., 1996). The resolution of the final map was estimated to be 25 Å, assuming a correlation coefficient cutoff of 0.5 in the Fourier shell correlation method (Baker et al., 1999). The resolution was rather limited because of the need to use far-from-focus micrographs to permit differentiation between partially mature particles (Zhang et al., 2004) and mature particles complexed with DC-SIGN CRD.

Fitting Atomic Structures of E into the cryoEM Map

The structure of the dimer as found in the mature DENV virion (PDB accession code 1THD) was fitted into the cryoEM map of the DENV-CRD complex. The fitting procedure was performed using the EMfit program (Rossmann et al., 2001), as described previously (Kuhn et al., 2002). Briefly, the icosahedral 2-fold dimer was first fitted by superimposing the dyad of the dimer onto the icosahedral 2-fold axis, allowing only the rotation around and the translation along the icosahedral 2-fold axis. The density corresponding to the icosahedral dimer was then set to zero before fitting the general dimer while refining three rotational and three translational parameters (Table 3).

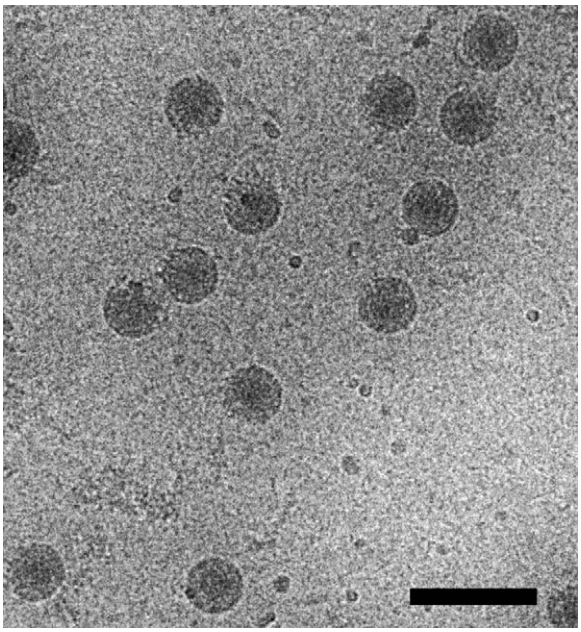

Figure 4. CryoEM Micrograph Showing Vitrified Water-Embedded DENV Complexed with DC-SIGN CRD

The image was taken with a defocus level of ~3 μm on a FEI CM300 microscope at a magnification of 33,000. The DENV was incubated with the DC-SIGN fragment for 12 hr at 4ºC. There was little evidence of any particle aggregation. The scale bar represents 1000 Å.

The radius of the mass center of the fitted E dimers was 5% less than that of the fitted E dimers in the 9.5 Å cryoEM map of mature DENV (Zhang et al., 2003a, 2004). This difference occurred because the images of the DENV-CRD complex were recorded with a different microscope and under a different magnification from images used for the mature DENV reconstruction. Therefore, the pixel size of the cryoEM map of the complex was increased by 5%. The fitting of E into the resultant, magnification-adjusted map of the complex was repeated, allowing for an accurate comparison of the E structures in the DENV-CRD complex and in the mature virus. The position of the carbohydrate moieties associated with the Asn67 and Asn153 residues was determined by moving the known crystal structure of the glycosylated E protein (PDB accession number 1OKE) into each of the E molecules that had been fitted into the cryoEM density (Zhang et al., 2004). These carbohydrate positions agree well with those found on the 9.5 Å resolution cryoEM map of DENV (Zhang et al., 2004).

Difference Map Calculation and Fitting of the CRD Atomic Structure

The difference map between the DENV-CRD complex and the mature DENV was computed in Fourier space using programs in CCP4 (Collaborative Computational Project, Number 4, 1994). Structure factors of both maps were calculated and scaled by minimizing the function $\sum[F_{complex} - kF_{DENV} \exp(-B\nu^2/4)]^2$ using data in the resolution range between 25 and 100 Å, where ν is the spatial frequency, k is a scale factor,

and B is a "temperature" factor. $F_{complex}$ and F_{DENV} are the structure amplitudes of the complex and mature DENV, respectively. The appropriate scaling between equivalent structure amplitudes results in a correlation coefficient of 0.81. The difference map of the complex minus the mature DENV was then computed by Fourier-transforming the vector differences between structure factors of the two data sets.

Crystal structures of DC-SIGN CRD and DC-SIGNR CRD were used to analyze the difference map. The initial determination was to establish whether the single difference peak per icosahedral asymmetric unit corresponded to one or two CRDs. Hence the fit of a single CRD (line 1 in Table 2) into the cryoEM density was compared to the fit of two closely packed CRDs. For the latter, two different crystal structures were used (PDB accession numbers 1K9I, chains A and B, and 1XAR, chains A and B) (lines 2 and 3 in Table 2, respectively). Both attempts at fitting two CRDs into the density produced a large percentage of atoms that were in negative density and, in the case of the 1K9I structure, there were extensive atomic clashes between icosahedrally related subunits. Thus, using a single monomer gave a significantly better fit to the density than the two attempts at fitting two molecules simultaneously. The oligosaccharide ligand of CRD in the crystal structures was omitted for the fitting. In order to obtain the best fit of the single monomer, the mass center of the pentasaccharide was restrained to lie within a 30 Å distance from each of the closest N-linked glycosylation sites of the corresponding E proteins. Attempts at more detailed modeling of the interaction between the CRD and the viral carbohydrate on the Asn67 residues were not justified in light of the lack of information about the nature of the carbohydrate conformation and uncertainty of the CRD's exact orientation.

ACKNOWLEDGMENTS

Figures were made using the program DINO (DINO: Visualizing Structural Biology, 2002, http://www.dino3d.org). We thank Wei Zhang for computing 14 Å and 25 Å resolution mature DENV cryoEM maps. We also thank Andrei Fokine for help with the cryoEM reconstructions and Shee-mei Lok for help in the ELISA experiment. We are grateful to Rob Ashmore and Victor Kostyuchenko for their various computer programs. We thank Sharon Wilder and Cheryl Towell for help in the preparation of the manuscript. The work was supported by an NIH Program Project grant to R.J.K. and M.G.R. (AI 55672), by an NIH grant to W.A.H. (AI40895), and a Keck Foundation grant to M.G.R. for the purchase of the CM300 electron microscope.

Received: August 22, 2005
Revised: October 6, 2005
Accepted: November 11, 2005
Published: February 9, 2006

REFERENCES

Baker, T.S., Olson, N.H., and Fuller, S.D. (1999). Adding the third dimension to virus life cycles: three-dimensional reconstruction of icosahedral viruses from cryo-electron micrographs. Microbiol. Mol. Biol. Rev. *63*, 862–922.

Bernhard, O.K., Lai, J., Wilkinson, J., Sheil, M.M., and Cunningham, A.L. (2004). Proteomic analysis of DC-SIGN on dendritic cells detects tetramers required for ligand binding but no association with CD4. J. Biol. Chem. *279*, 51828–51835.

Bewley, M.C., Springer, K., Zhang, Y.B., Freimuth, P., and Flanagan, J.M. (1999). Structural analysis of the mechanism of adenovirus binding to its human cellular receptor, CAR. Science *286*, 1579–1583.

Bhardwaj, S., Holbrook, M., Shope, R.E., Barrett, A.D.T., and Watowich, S.J. (2001). Biophysical characterization and vector-specific antagonist activity of domain III of the tick-borne flavivirus envelope protein. J. Virol. *75*, 4002–4007.

Bhella, D., Goodfellow, I.G., Roversi, P., Chaudhry, Y., Evans, D.J., and Lea, S.M. (2004). The structure of echovirus type 12 bound to a two-domain fragment of its cellular attachment protein decay-accelerating factor (CD55). J. Biol. Chem. *279*, 8325–8332.

Burmeister, W.P., Guilligay, D., Cusack, S., Wadell, G., and Arnberg, N. (2004). Crystal structure of species D adenovirus fiber knobs and their sialic acid binding sites. J. Virol. *78*, 7727–7736.

Cambi, A., and Figdor, C.G. (2003). Dual function of C-type lectin-like receptors in the immune system. Curr. Opin. Cell Biol. *15*, 539–546.

Carfi, A., Willis, S.H., Whitbeck, J.C., Krummenacher, C., Cohen, G.H., Eisenberg, R.J., and Wiley, D.C. (2001). Herpes simplex virus glycoprotein D bound to the human receptor HveA. Mol. Cell *8*, 169–179.

Caspar, D.L.D., and Klug, A. (1962). Physical principles in the construction of regular viruses. Cold Spring Harb. Symp. Quant. Biol. *27*, 1–24.

CCP4 (Collaborative Computational Project, Number 4) (1994). The CCP4 suite: programs for protein crystallography. Acta Crystallogr. D *50*, 760–763.

Conway, J.F., and Steven, A.C. (1999). Methods for reconstructing density maps of "single" particles from cryoelectron micrographs to subnanometer resolution. J. Struct. Biol. *128*, 106–118.

Feinberg, H., Mitchell, D.A., Drickamer, K., and Weis, W.I. (2001). Structural basis for selective recognition of oligosaccharides by DC-SIGN and DC-SIGNR. Science *294*, 2163–2166.

Feinberg, H., Guo, Y., Mitchell, D.A., Drickamer, K., and Weis, W.I. (2005). Extended neck regions stabilize tetramers of the receptors DC-SIGN and DC-SIGNR. J. Biol. Chem. *280*, 1327–1335.

Frank, J., Radermacher, M., Penczek, P., Zhu, J., Li, Y., Ladjadj, M., and Leith, A. (1996). SPIDER and WEB: processing and visualization of images in 3D electron microscopy and related fields. J. Struct. Biol. *116*, 190–199.

Guo, Y., Feinberg, H., Conroy, E., Mitchell, D.A., Alvarez, R., Blixt, O., Taylor, M.E., Weis, W.I., and Drickamer, K. (2004). Structural basis for distinct ligand-binding and targeting properties of the receptors DC-SIGN and DC-SIGNR. Nat. Struct. Mol. Biol. *11*, 591–598.

He, Y., Lin, F., Chipman, P.R., Bator, C.M., Baker, T.S., Shoham, M., Kuhn, R.J., Medof, M.E., and Rossmann, M.G. (2002). Structure of decay-accelerating factor bound to echovirus 7: a virus-receptor complex. Proc. Natl. Acad. Sci. U.S. *99*, 10325–10329.

Johnson, A.J., Guirakhoo, F., and Roehrig, J.T. (1994). The envelope glycoproteins of dengue 1 and dengue 2 viruses grown in mosquito cells differ in their utilization of potential glycosylation sites. Virology *203*, 241–249.

Kuhn, R.J., Zhang, W., Rossmann, M.G., Pletnev, S.V., Corver, J., Lenches, E., Jones, C.T., Mukhopadhyay, S., Chipman, P.R., Strauss, E.G., et al. (2002). Structure of dengue virus: implications for flavivirus organization, maturation, and fusion. Cell *108*, 717–725.

Kwong, P.D., Wyatt, R., Robinson, J., Sweet, R.W., Sodroski, J., and Hendrickson, W.A. (1998). Structure of an HIV gp120 envelope glycoprotein in complex with the CD4 receptor and a neutralizing human antibody. Nature *393*, 648–659.

Lindenbach, B.D., and Rice, C.M. (2001). *Flaviviridae*: the viruses and their replication. In Fields Virology, D.M. Knipe, and P.M. Howley, eds. (Philadelphia: Lippincott Williams & Wilkins), pp. 991–1041.

Lozach, P.-Y., Lortat-Jacob, H., De Lacroix De Lavalette, A., Staropoli, I., Foung, S., Amara, A., Houlès, C., Fieschi, F., Schwartz, O., Virelizier, J.-L., et al. (2003). DC-SIGN and L-SIGN are high affinity binding receptors for hepatitis C virus glycoprotein E2. J. Biol. Chem. *278*, 20358–20366.

Lozach, P.-Y., Burleigh, L., Staropoli, I., Navarro-Sanchez, E., Harriague, J., Virelizier, J.-L., Rey, F.A., Desprès, P., Arenzanz-Seisdedos, F., and Amara, A. (2005). Dendritic cell-specific intercellular adhesion molecule 3-grabbing non-integrin (DC-SIGN)–mediated enhancement of dengue virus infection is independent of DC-SIGN internalization signals. J. Biol. Chem. *280*, 23698–23708.

Mitchell, D.A., Fadden, A.J., and Drickamer, K. (2001). A novel mechanism of carbohydrate recognition by the C-type lectins DC-SIGN and DC-SIGNR. Subunit organization and binding to multivalent ligands. J. Biol. Chem. *276*, 28939–28945.

Modis, Y., Ogata, S., Clements, D., and Harrison, S.C. (2003). A ligand-binding pocket in the dengue virus envelope glycoprotein. Proc. Natl. Acad. Sci. U.S. *100*, 6986–6991.

Morens, D.M. (1994). Antibody-dependent enhancement of infection and the pathogenesis of viral disease. Clin. Infect. Dis. *19*, 500–512.

Mukhopadhyay, S., Kim, B.-S., Chipman, P.R., Rossmann, M.G., and Kuhn, R.J. (2003). Structure of West Nile virus. Science *302*, 248.

Navarro-Sanchez, E., Altmeyer, R., Amara, A., Schwartz, O., Fieschi, F., Virelizier, J.-L., Arenzana-Seisdedos, F., and Desprès, P. (2003). Dendritic-cell-specific ICAM3-grabbing non-integrin is essential for the productive infection of human dendritic cells by mosquito-cell-derived dengue viruses. EMBO Rep. *4*, 723–728.

Pletnev, S.V., Zhang, W., Mukhopadhyay, S., Fisher, B.R., Hernandez, R., Brown, D.T., Baker, T.S., Rossmann, M.G., and Kuhn, R.J. (2001). Locations of carbohydrate sites on Sindbis virus glycoproteins show that E1 forms an icosahedral scaffold. Cell *105*, 127–136.

Rey, F.A., Heinz, F.X., Mandl, C., Kunz, C., and Harrison, S.C. (1995). The envelope glycoprotein from tick-borne encephalitis virus at 2 Å resolution. Nature *375*, 291–298.

Rossmann, M.G. (1994). Viral cell recognition and entry. Protein Sci. *3*, 1712–1725.

Rossmann, M.G., Arnold, E., Erickson, J.W., Frankenberger, E.A., Griffith, J.P., Hecht, H.J., Johnson, J.E., Kamer, G., Luo, M., Mosser, A.G., et al. (1985). Structure of a human common cold virus and functional relationship to other picornaviruses. Nature *317*, 145–153.

Rossmann, M.G., Bernal, R., and Pletnev, S.V. (2001). Combining electron microscopic with X-ray crystallographic structures. J. Struct. Biol. *136*, 190–200.

Rossmann, M.G., He, Y., and Kuhn, R.J. (2002). Picornavirus-receptor interactions. Trends Microbiol. *10*, 324–331.

Snyder, G.A., Colonna, M., and Sun, P.D. (2005). The structure of DC-SIGNR with a portion of its repeat domain lends insights to modeling of the receptor tetramer. J. Mol. Biol. *347*, 979–989.

Stehle, T., and Harrison, S.C. (1996). Crystal structures of murine polyomavirus in complex with straight-chain and branched-chain sialyloligosaccharide receptor fragments. Structure *4*, 183–194.

Stehle, T., and Harrison, S.C. (1997). High-resolution structure of a polyomavirus VP1-oligosaccharide complex: implications for assembly and receptor binding. EMBO J. *16*, 5139–5148.

Su, S.V., Hong, P., Baik, S., Negrete, O.A., Gurney, K.B., and Lee, B. (2004). DC-SIGN binds to HIV-1 glycoprotein 120 in a distinct but overlapping fashion compared with ICAM-2 and ICAM-3. J. Biol. Chem. *279*, 19122–19132.

Tassaneetrithep, B., Burgess, T., Granelli-Piperno, A., Trumpfheller, C., Finke, J., Sun, W., Eller, M., Pattanapanyasat, K., Sarasombath, S., Birx, D., et al. (2003). DC-SIGN (CD209) mediates dengue virus infection of human dendritic cells. J. Exp. Med. *197*, 823–829.

Verdaguer, N., Fita, I., Reithmayer, M., Moser, R., and Blaas, D. (2004). X-ray structure of a minor group human rhinovirus bound to a fragment of its cellular receptor protein. Nat. Struct. Mol. Biol. *11*, 429–434.

Weis, W.I., Kahn, R., Fourme, R., Drickamer, K., and Hendrickson, W.A. (1991). Structure of the calcium-dependent lectin domain from a rat mannose-binding protein determined by MAD phasing. Science *254*, 1608–1615.

Wu, S.J., Grouard-Vogel, G., Sun, W., Mascola, J.R., Brachtel, E., Putvatana, R., Louder, M.K., Filgueira, L., Marovich, M.A., Wong, H.K., et al. (2000). Human skin Langerhans cells are targets of dengue virus infection. Nat. Med. *6*, 816–820.

Zhang, W., Chipman, P.R., Corver, J., Johnson, P.R., Zhang, Y., Mukhopadhyay, S., Baker, T.S., Strauss, J.H., Rossmann, M.G., and Kuhn, R.J. (2003a). Visualization of membrane protein domains in flavivirus virions. Nat. Struct. Biol. *10*, 907–912.

Zhang, Y., Corver, J., Chipman, P.R., Zhang, W., Pletnev, S.V., Sedlak, D., Baker, T.S., Strauss, J.H., Kuhn, R.J., and Rossmann, M.G. (2003b). Structures of immature flavivirus particles. EMBO J. *22*, 2604–2613.

Zhang, Y., Zhang, W., Ogata, S., Clements, D., Strauss, J.H., Baker, T.S., Kuhn, R.J., and Rossmann, M.G. (2004). Conformational changes of the flavivirus E glycoprotein. Structure *12*, 1607–1618.

Accession Numbers

The cryo-EM map of the DENV-CRD complex and the difference map were deposited with the EBI (accession number EMD1166 and EMD1167, respectively), and the coordinates of the fitted CRD were deposited with the Protein Data Bank (accession number 2B6B).